This article has been accepted for publication in a future issue of this journal, but has not been fully edited. Content may change prior to final publication. Citation information: DOI 10.1109/TIE.2014.2316239, IEEE Transactions on Industrial Electronics

Position Control of the Induction Motor Using an Adaptive Sliding Mode Controller and Observers

Oscar Barambones, *Senior Member, IEEE,* and Patxi Alkorta, *Member, IEEE,*

***Abstract*—An adaptive robust position control for real time high-performance applications of induction motors is developed in this work. The proposed sliding mode controller provides a global asymptotic position tracking in the presence of model uncertainties and load torque variations. The proposed control scheme incorporates an adaptation law for the switching gain, so that the controller can calculate the switching gain value that is necessary to overcome the existing system uncertainties. The design also incorporates a sliding mode based load torque and rotor flux observers in order to improve the control performance without using sensors that increases the cost and reduces the reliability. The proposed design does not present a high computational cost and therefore can be implemented easily in the real time applications. Simulated and experimental results show that this scheme provides a high-performance dynamic characteristics and that is robust with respect to plant parameter variations and external load disturbances.**

***Index Terms*—Induction Motor, Field-oriented control, Position Control, Sliding Mode Observer and Control.**

I. Introduction

Induction motors (IM) have been widely used in industrial applications such as machine tools, steel mills and paper machines, owing to their good performance provided by their solid architecture, low moment of inertia, low ripple of torque and high initiated torque. In order to regulate the IM in high-performance applications several control techniques have been developed being the field oriented control method [1] one of the most popular techniques.

The field oriented technique decouples torque and flux control commands for the IM, but the control performance of the resulting system is still influenced by uncertainties, which usually are composed of unpredictable parameter variations, external load disturbances, and unmodelled and nonlinear dynamics. Therefore, many studies have been made on the motor drives in order to preserve the performance under these parameter variations and external load disturbances, such as, predictive control [2], [3], adaptive control [4], robust control [5], fuzzy control [6] and direct torque control [7]. The Sliding Mode Control is a nonlinear robust control that can overcome the model uncertainties and external disturbances, and thereby it is very attractive for IM control [10].

Position control is often used in some applications of electrical drives like robotic systems, conveyor belts, etc. In these applications, traditionally DC motors are used due to their linear behavior. However, the squirrel cage induction motor presents some excellent constructional features such as reliability, high efficiency, ruggedness, low cost, and low maintenance, which make the use of an IM very attractive for some applications. However, due to their highly coupled nonlinear structure, the IM position control presents some drawbacks that should be solved using more sophisticated controllers [11]. In these applications uncertainty and external disturbances are also present and therefore a robust control system that maintain the desired control performance under these situations are frequently required. In this sense, during the last years, the sliding mode control has been focussed on many studies and research for the position control of the induction motors [12]-[14]. In the work presented in [12] the induction motor position control problem has been studied using a discrete time sliding mode control. However in this work the authors, should select the switching gain, taking into account the system uncertainties, in order to obtain the convergence to the sliding surface. Moreover, in this work the authors also calculate the angular position of the rotor flux vector in an open loop using the slip estimate which is very sensitive to the parameter uncertainties. In this sense this control scheme can be improved using a rotor flux observer in order to calculate the angular position of the rotor flux vector, and employing an adaptive switching gain in the controller as it is proposed in this work. In the paper [14] the authors present a robust position control for IM but in this work a Luenberger observer is used which is sensitive to the model uncertainties and in this work experimental results using a commercial IM are not presented.

On the other hand, the sensors increase the cost and also reduce the reliability of the control system because these elements are generally expensive, delicate and difficult to install. Therefore, considerable efforts should be made to reduce the number of sensors in the control systems [15],[16]. Recently a novel estimators for induction motor has been proposed in [17] and [18]. In [17] the measured stator current of the IM, used as a reference signal, is compared with the stator current estimated using the stator voltage-current model. However in this paper the rotor flux is calculated using the current model of the rotor flux without including any corrector terms in order to compensate the model uncertainties. In [18], an state estimation of induction motor drives using the unscented Kalman filter is proposed, however the proposed

Manuscript received September 25, 2013; revised December 23, 2013 and February 10, 2014; accepted March 20,2014.

This work was supported in part by the Basque Government through the project S-PE12UN015 and by the University of the Basque Country through the projects GIU13/41 and UFI11/07.

O. Barambones is with the Vitoria Engineering School, University of the Basque Country. e-mail: oscar.barambones@ehu.es

P. Alkorta is with the Eibar Engineering School, University of the Basque Country. e-mail: patxi.alkorta@ehu.es

This article has been accepted for publication in a future issue of this journal, but has not been fully edited. Content may change prior to final publication. Citation information: DOI 10.1109/TIE.2014.2316239, IEEE Transactions on Industrial Electronics

Kalman filter presents a high computational cost, which can be undesirable in order to implement this observer in commercial applications.

In order to overcome these problems a Sliding Mode Observer (SMO) is proposed in this paper. The proposed SMO unlike the observer proposed in [19]-[20] also incorporates a proportional current error term, in order to reduce the observer sliding gain value and thus to improve the observer behavior. Moreover, the proposed observer presents a low computational cost and therefore this observer is adequate to be implemented in the induction motor control real time applications for industrial purposes.

In this paper a new observer-controller scheme that incorporates an adaptive robust position control and a robust rotor flux and load torque estimator for high-performance IM applications is proposed. The overall control scheme does not involve a high computational cost and therefore can be implemented in real time applications using a low cost processors. The main contributions of this paper can be summarized as follow: The paper introduces an adaptive robust approach for induction motor position control, that overcomes the system uncertainties and load disturbances that are usually present in real systems. The proposed design incorporates an adaptation law for the sliding gain so that the sliding mode controller can adapt the sliding gain value that is necessary to overcome the existing system uncertainties. In this sense, the control signal of the proposed sliding mode control scheme will be smaller than the control signals of the traditional sliding mode control schemes [8],[12], because in the latter, the sliding gain value should be chosen high enough to overcome all the possible uncertainties that could appear in the system over the time. However, in our scheme, the sliding gain value is small when the system uncertainties are small, and if the system uncertainties increase the sliding gain value is increased (if necessary) to overcome this increment in the system uncertainties. Besides, in order to reduce the load torque uncertainties, a sliding mode load torque observer is proposed. The load torque observer improves the position control performance because reduces the system uncertainties and therefore reduces the sliding gain value that is necessary in order to get the attractivity condition towards the sliding surface. Furthermore, a sliding mode flux observer is proposed in order to avoid the flux sensors for calculating the rotor flux vector angular position, whose value is essential in order to apply the field oriented control principle. This observer presents a robust performance and a low computational cost. Finally, the proposed control scheme is validated in a real test, using a commercial induction motor, in order to demonstrate the real performance of this controller. The experimental validation has been implemented using a control platform based on a DS1103 PPC Controller Board that has been designed and constructed for this purpose.

II. Sliding mode observer for rotor flux estimator

From singular perturbation theory [21], and based on the well-known IM model dynamics, the slow variables of the system are ψ_{dr}, ψ_{qr} and the fast variables are i_{ds}, i_{qs}. Therefore, the corresponding singularly perturbed model of the IM using the d-q stationary reference frame is:

$$\begin{aligned}
\varepsilon\dot{i}_{ds} &= -L_m\alpha_r i_{ds} + \alpha_r\psi_{dr} + w_r\psi_{qr} + \frac{L_r}{L_m}(V_{ds} - R_s i_{ds}) \\
\varepsilon\dot{i}_{qs} &= -L_m\alpha_r i_{qs} - w_r\psi_{dr} + \alpha_r\psi_{qr} + \frac{L_r}{L_m}(V_{qs} - R_s i_{qs}) \\
\dot{\psi}_{dr} &= L_m\alpha_r i_{ds} - \alpha_r\psi_{dr} - w_r\psi_{qr} \\
\dot{\psi}_{qr} &= L_m\alpha_r i_{qs} + w_r\psi_{dr} - \alpha_r\psi_{qr}
\end{aligned} \tag{1}$$

where V_{ds}, V_{qs} are stator voltages; i_{ds}, i_{qs} are stator currents; ψ_{dr}, ψ_{qr} are rotor fluxes; w_r is motor speed; R_s, R_r are stator and rotor resistances; L_s, L_r are stator and rotor inductances; L_m, is mutual inductance; $\sigma = 1 - \frac{L_m^2}{L_s L_r}$ is leakage coefficient; $T_r = \frac{L_r}{R_r}$ is rotor-time constant; $\varepsilon = \frac{\sigma L_s L_r}{L_m}$; $\alpha_r = \frac{1}{T_r}$.

Using the system model (1), the proposed sliding mode observer can be designed as follows:

$$\begin{aligned}
\varepsilon\dot{\hat{i}}_{ds} &= -L_m\alpha_r i_{ds} + \alpha_r\hat{\psi}_{dr} + w_r\hat{\psi}_{qr} + \frac{L_r}{L_m}(V_{ds} - R_s i_{ds}) \\
&\quad + k_1 e_{i_d} - g_{i_d}\,\mathrm{sgn}(e_{id}) \\
\varepsilon\dot{\hat{i}}_{qs} &= -L_m\alpha_r i_{qs} - w_r\hat{\psi}_{dr} + \alpha_r\hat{\psi}_{qr} + \frac{L_r}{L_m}(V_{qs} - R_s i_{qs}) \\
&\quad + k_2 e_{iq} - g_{i_q}\,\mathrm{sgn}(e_{iq}) \\
\dot{\hat{\psi}}_{dr} &= L_m\alpha_r i_{ds} - \alpha_r\hat{\psi}_{dr} - w_r\hat{\psi}_{qr} - g_{\psi_d}\,\mathrm{sgn}(e_{id}) \\
\dot{\hat{\psi}}_{qr} &= L_m\alpha_r i_{qs} + w_r\hat{\psi}_{dr} - \alpha_r\hat{\psi}_{qr} - g_{\psi_q}\,\mathrm{sgn}(e_{iq})
\end{aligned} \tag{2}$$

where $\hat{i}$ and $\hat{\psi}$ are the estimations of i and ψ; k_1, k_2, g_{i_d}, g_{i_q}, g_{ψ_d} and g_{ψ_q} are the observer gains; $e_{i_d} = i_{ds} - \hat{i}_{ds}$ and $e_{i_q} = i_{qs} - \hat{i}_{qs}$ are the current estimation errors; $\mathrm{sgn}()$ is the sign function.

Subtracting (2) from (1), the estimation error dynamics can be expressed in matrix form as:

$$\begin{aligned}
\varepsilon\dot{e}_i &= +Ae_\psi + K_i e_i + G_i\Upsilon_e \\
\dot{e}_\psi &= -Ae_\psi + G_\psi\Upsilon_e
\end{aligned} \tag{3}$$

where $e_{\psi_d} = \psi_{dr} - \hat{\psi}_{dr}$, $e_{\psi_q} = \psi_{qr} - \hat{\psi}_{qr}$ are the flux estimation errors, $A = \alpha_r I_2 - w_r J_2$, $e_i = [e_{i_d}\ \ e_{i_q}]^T$, $e_\psi = [e_{\psi_d}\ e_{\psi_q}]^T$, $\Upsilon_e = [\mathrm{sgn}(e_{id})\ \ \mathrm{sgn}(e_{iq})]^T$,

$$G_i = \begin{bmatrix} g_{i_d} & 0 \\ 0 & g_{i_q} \end{bmatrix}, G_\psi = \begin{bmatrix} g_{\psi_d} & 0 \\ 0 & g_{\psi_q} \end{bmatrix}$$

$$I_2 = \begin{bmatrix} 1 & 0 \\ 0 & 1 \end{bmatrix}, J_2 = \begin{bmatrix} 0 & -1 \\ 1 & 0 \end{bmatrix}, K_i = \begin{bmatrix} -k_1 & 0 \\ 0 & -k_2 \end{bmatrix}$$

The stability analysis of this system can be considered using the two-time-scale approach. Then, first the observer gains G_i and K_i of the fast subsystem (i_{ds}, i_{qs}) are determined to ensure the attractiveness of the sliding surface $e_i = 0$ in the fast time scale. Thereafter, the observer gain G_ψ of the slow subsystem (ψ_{dr}, ψ_{qr}), are determined, such that the reduced-order system (obtained when $e_i \cong \dot{e}_i \cong 0$) is locally stable [21].

The fast subsystem of (3) can be obtained by introducing the new time variable $\tau = (t - t_0)/\varepsilon$ and thereafter setting $\varepsilon \to 0$ [21]. In the new time scale τ, taking into account that

This article has been accepted for publication in a future issue of this journal, but has not been fully edited. Content may change prior to final publication. Citation information: DOI 10.1109/TIE.2014.2316239, IEEE Transactions on Industrial Electronics

$d\tau = dt/\varepsilon$, from (3) it is obtained:

$$\begin{aligned} \frac{d}{d\tau}e_i &= Ae_\psi + K_i e_i + G_i \Upsilon_e \\ \frac{d}{d\tau}e_\psi &= 0 \end{aligned} \quad (4)$$

Therefore, if the observer gains G_i and K_i are adequately chosen, the sliding mode occurs in (4) along the manifold $e_i = [e_{i_d}\ e_{i_q}]^T = 0$.

Proof: Let us define the following Lyapunov function candidate,

$$V = \frac{1}{2}e_i^T e_i$$

whose time derivative is,

$$\begin{aligned} \frac{dV}{d\tau} &= e_i^T \frac{de_i}{d\tau} = e_i^T[Ae_\psi + K_i e_i + G_i\Upsilon_e] \quad (5) \\ &= \begin{bmatrix} e_{id}\left\{g_{i_d}\,\mathrm{sgn}(e_{id}) + \alpha_r e_{\psi_d} + w_r e_{\psi_q} - k_1 e_{id}\right\} \\ e_{iq}\left\{g_{i_q}\,\mathrm{sgn}(e_{iq}) - w_r e_{\psi_d} + \alpha_r e_{\psi_q} - k_2 e_{iq}\right\} \end{bmatrix} \end{aligned}$$

Then, the attractivity condition is fulfilled selecting a sufficiently large negative numbers g_{i_d}, g_{i_q}, and positive numbers k_1 and k_2 in order to satisfy the following inequalities:

$$\begin{aligned} g_{i_d} &< -\left|\alpha_r e_{\psi_d} + w_r e_{\psi_q}\right| + k_1\left|e_{id}\right| \\ g_{i_q} &< -\left|-w_r e_{\psi_d} + \alpha_r e_{\psi_q}\right| + k_2\left|e_{iq}\right| \end{aligned} \quad (6)$$

When the currents trajectory reaches the sliding surface $e_i = 0$, the observer error dynamics given by (3) behaves, in the sliding mode, as a reduced order system governed only by the rotor flux error e_ψ, because $e_i = \dot{e}_i = 0$:

$$\begin{aligned} 0 &= +Ae_\psi + G_i\Upsilon_e \\ \dot{e}_\psi &= -Ae_\psi + G_\psi\Upsilon_e \end{aligned} \quad (7)$$

In order to demonstrate the stability of the previous system, the following Lyapunov function candidate is proposed:

$$V = \frac{1}{2}e_\psi^T e_\psi \quad (8)$$

The time derivative of the Lyapunov function candidate is:

$$\begin{aligned} \frac{dV}{dt} &= \dot{e}_\psi^T e_\psi = -\Upsilon_e^T (G_i + G_\psi)^T A^{-1} G_i \Upsilon_e \\ &= -\Upsilon_e^T \left[(I_2 + G_\psi G_i^{-1})G_i\right]^T A^{-1} G_i \Upsilon_e \\ &= -\Upsilon_e^T G_i^T (I_2 + G_\psi G_i^{-1})^T A^{-1} G_i \Upsilon_e \\ &= -\Upsilon_e^T G_i^T (A^{-1})^T A^T (I_2 + G_\psi G_i^{-1})^T A^{-1} G_i \Upsilon_e \\ &= -(A^{-1}G_i\Upsilon_e)^T A^T (I_2 + G_\psi G_i^{-1})^T A^{-1} G_i \Upsilon_e \\ &= -e_\psi^T A^T (I_2 + G_\psi G_i^{-1})^T e_\psi \\ &= -e_\psi (I_2 + G_\psi G_i^{-1}) A\, e_\psi^T \end{aligned} \quad (9)$$

To ensure that $\dot{V}$ is negative definite the following sufficient condition can be requested:

$$(I_2 + G_\psi G_i^{-1})A \geq \varrho I_2\ , \quad \varrho > 0 \quad (10)$$

Solving the gain matrix G_ψ in (10) yields:

$$G_\psi \leq (\varrho A^{-1} - I_2)G_i \quad (11)$$

Therefore, the time derivative of the Lyapunov function will be negative definite if the observer gain G_ψ is chosen taking into account (11). As a result from (9) it is concluded that the equilibrium point ($e_\psi = 0$) of the flux observer error dynamic given by (7) is exponentially stable; that is, the flux observer error converges to zero with exponential rate of convergence.

III. Sliding Mode Load Torque Observer

When the load torque is unknown or it is very variable over time, the load toque should be considered as a system uncertainty and then the control system should be robust under this uncertainty. In this paper a sliding mode load torque estimator is proposed in order to reduce this system uncertainty and improve the control performance.

The well known induction motor mechanical equation is:

$$J\ddot{\theta}_m + B\dot{\theta}_m + T_L = T_e \quad (12)$$

where J is the inertia constant; B is the viscous friction coefficient; T_L is the external load; θ_m is the rotor mechanical position, which is related to the rotor electrical position, θ_r, by $\theta_m = 2\,\theta_r/p$ where p is the pole numbers.

Using the field-orientation control principle $\psi_{qr}^e = 0$ and $\psi_{dr}^e = |\bar{\psi}_r|$, so the induction motor torque T_e is simplified to:

$$T_e = \frac{3p}{4}\frac{L_m}{L_r}\psi_{dr}^e i_{qs}^e = K_T\, i_{qs}^e \quad (13)$$

where ψ_{dr}^e and ψ_{qr}^e are the rotor-flux linkages, i_{ds}^e, i_{qs}^e are the stator current components, and the subscript 'e' indicates that are referred to the synchronously rotating reference frame.

The dynamic equation of the IM is obtained using the mechanical equation (12) and the torque equation (13) :

$$\dot{w}_m = -\frac{B}{J}w_m + \frac{K_T}{J}\, i_{qs}^e - \frac{1}{J}T_L \quad (14)$$

The load torque can be considered as a quasi-constant signal assuming that it only changes at certain instants. Accordingly, the system state space equations are:

$$\begin{aligned} \dot{w}_m &= -\frac{B}{J}w_m + \frac{K_T}{J}\, i_{qs}^e - \frac{1}{J}T_L \\ \dot{T}_L &= 0 \end{aligned} \quad (15)$$

Taking into account that the load torque T_L is taken as a quasi-constant signal, the load torque can be considered the slow component of this system. Therefore, from singular perturbation theory [21], the stability can be demonstrated assuring the asymptotic stability of the fast component of this system (the rotor speed), and thereafter the convergence of the slow component (the load torque) for the reduced system, when the rotor speed estimation error is zero.

The proposed SM observer is:

$$\begin{aligned} \dot{\hat{w}}_m &= \frac{-B}{J}w_m + \frac{K_T}{J}i_{qs}^e - \frac{1}{J}\hat{T}_L + k_{w_1}e_w + h_1\,\mathrm{sgn}(e_w) \\ \dot{\hat{T}}_L &= -k_{w_2}e_w - h_2\,\mathrm{sgn}(e_w) \end{aligned} \quad (16)$$

where $e_w = w_m - \hat{w}_m$, and k_{w_1}, k_{w_2}, h_1 and h_2 are a positive constants.

From (16) and (15) the estimation error is obtained:

$$\begin{aligned} \dot{e}_w &= -\frac{1}{J}e_T - k_{w_1}e_w - h_1\,\mathrm{sgn}(e_w) \\ \dot{e}_T &= k_{w_2}e_w + h_2\,\mathrm{sgn}(e_w) \end{aligned} \quad (17)$$

This article has been accepted for publication in a future issue of this journal, but has not been fully edited. Content may change prior to final publication. Citation information: DOI 10.1109/TIE.2014.2316239, IEEE Transactions on Industrial Electronics

where $e_T = T_L - \hat{T}_L$

In order to demonstrate the stability of the fast component the following Lyapunov function candidate is proposed:

$$V = \frac{1}{2} e_w^2 \tag{18}$$

The time derivative of this Lyapunov function candidate is:

$$\begin{aligned} \dot{V} &= e_w \dot{e}_w && (19)\\ &= e_w \left(-\frac{1}{J} e_T - k_{w_1} e_w - h_1 \operatorname{sgn}(e_w) \right) && (20)\\ &= -h_1 |e_w| - k_{w_1} e_w^2 - \frac{1}{J} e_w e_T && (21) \end{aligned}$$

To ensure that $\dot{V}$ is negative definite the following sufficient condition can be requested:

$$h_1 \geq \left| \frac{1}{J} e_T \right| - k_{w_1} |e_w| + \eta_w \ , \quad \eta_w > 0 \tag{22}$$

Therefore,

$$\dot{V} \leq -\eta_w |e_w| \tag{23}$$

From (23) it is deduced that the equilibrium point $e_w = 0$ is asymptotically stable, and from this equation it can be also deduced that the maximum time in order to reach the equilibrium point $e_w = 0$ is:

$$t_{reach} \leq \frac{e_w(t=0)}{\eta_w} \tag{24}$$

When the speed observation error reaches the equilibrium point, $e_w = 0$ and $\dot{e}_w = 0$, and then from (17) it is obtained that the observer error dynamics behaves as the reduced-order subsystem presented below:

$$\begin{aligned} 0 &= -\frac{1}{J} e_T - h_1 \operatorname{sgn}(e_w) && (25)\\ \dot{e}_T &= h_2 \operatorname{sgn}(e_w) && (26) \end{aligned}$$

From the previous equations it is obtained:

$$\dot{e}_T = -\frac{1}{J} \frac{h_2}{h_1} e_T \tag{27}$$

and therefore e_T converges to zero.

Therefore, the estimation error converges to zero if the observer gains h_1, h_2 k_{w_1} and k_{w_2} are selected taking into account the conditions given after eqn.(16) and eqn.(22). Accordingly the estimated states $\hat{w}_m$, $\hat{T}_L$ converges to the real states w_m, T_L as t tends to infinity, and the load torque may be obtained from the sliding mode observer given by (16).

IV. Adaptive sliding mode position control

Taking into account the system uncertainties, from (14), the dynamic equation of an induction motor can be written as [14]:

$$\ddot{\theta}_m = -(a + \triangle a)\dot{\theta}_m - (f + \triangle f) + (b + \triangle b) i_{qs}^e \tag{28}$$

where the terms a, b and f are:

$$a = \frac{B}{J}, \quad b = \frac{K_T}{J}, \quad f = \frac{\hat{T}_L}{J}; \tag{29}$$

and the uncertainties in the values of a, b and f are represented by the terms $\triangle a$, $\triangle b$ and $\triangle f$ respectively.

The position tracking error is defined as follows:

$$e(t) = \theta_m(t) - \theta_m^*(t) \tag{30}$$

where θ_m^* is the rotor position command.

The second derivative of (30) is:

$$\ddot{e}(t) = \ddot{\theta}_m - \ddot{\theta}_m^* = -a\, \dot{e}(t) + u(t) + d(t) \tag{31}$$

where the signal $u(t)$ collects the terms:

$$u(t) = b\, i_{qs}^e(t) - a\, \dot{\theta}_m^*(t) - f(t) - \ddot{\theta}_m^*(t) \tag{32}$$

and the signal $d(t)$ collects the uncertainty terms:

$$d(t) = -\triangle a\, w_m(t) - \triangle f(t) + \triangle b\, i_{qs}^e(t) \tag{33}$$

The sliding variable $S(t)$ is defined as:

$$S(t) = \dot{e}(t) + k\, e(t) \tag{34}$$

where k is a positive constant gain.

The proposed adaptive sliding mode position control law is:

$$u(t) = -(k - a)\, \dot{e}(t) - \hat{\beta} \gamma \operatorname{sgn}(S) \tag{35}$$

where $\hat{\beta}$ is the adaptive switching gain and $\operatorname{sgn}(\cdot)$ is the sign function.

The switching gain $\hat{\beta}$ is updated by means of the next adaptation law:

$$\dot{\hat{\beta}}(t) = \gamma\, |S(t)| \qquad \hat{\beta}(0) = 0 \tag{36}$$

where the positive constant γ can be used to select the adaptation speed.

The control law (35) with the adaptation law (36) leads the rotor mechanical position $\theta_m(t)$ so that the position tracking error $e(t) = \theta_m(t) - \theta_m^*(t)$ tends to zero as the time tends to infinity, and the proof is carried out using the Lyapunov stability theory.

$$V(t) = \frac{1}{2} S(t) S(t) + \frac{1}{2} \tilde{\beta}(t) \tilde{\beta}(t) \tag{37}$$

where $\tilde{\beta}(t) = \hat{\beta}(t) - \beta$, and $\beta \geq d_{max} + \eta$

The derivative of $V(t)$ is:

$$\begin{aligned} \dot{V}(t) = \ & S(t)\dot{S}(t) + \tilde{\beta}(t)\dot{\tilde{\beta}}(t) = S \cdot [\ddot{e} + k\, \dot{e}] + \tilde{\beta}\dot{\tilde{\beta}}\\ &= S \cdot [(-a\, \dot{e} + u + d) + k\, \dot{e}] + \tilde{\beta}\, \gamma |S|\\ &= S \cdot \left[-\hat{\beta} \gamma \operatorname{sgn}(S) + d \right] + (\hat{\beta} - \beta)\gamma |S|\\ &= d\, S - \hat{\beta}\gamma |S| + \hat{\beta}\gamma |S| - \beta \gamma |S| && (38)\\ &\leq |d||S| - (d_{max} + \eta)\gamma |S|\\ &\leq -\eta\, \gamma |S| \leq 0 && (39) \end{aligned}$$

Considering that $\dot{V}(t)$ is negative semidefinite, $V(t)$ is positive-definite and that when $S(t)$ and $\tilde{\beta}(t)$ tends to infinity $V(t)$ also tends to infinity, then the origin $[S(t), \tilde{\beta}(t)] = [0, 0]$ is a globally stable equilibrium point and consequently the terms $S(t)$ and $\tilde{\beta}(t)$ are bounded. Taking into account that $S(t)$ is bounded it is concluded that $e(t)$ and $\dot{e}(t)$ are also bounded.

This article has been accepted for publication in a future issue of this journal, but has not been fully edited. Content may change prior to final publication. Citation information: DOI 10.1109/TIE.2014.2316239, IEEE Transactions on Industrial Electronics

The derivative of the sliding variable (34) is:

$$\dot{S}(t) = \ddot{e}(t) + k\dot{e}(t) \tag{40}$$

then, using (31) and (35) is obtained

$$\begin{aligned} \dot{S}(t) &= -a\dot{e}(t) + u(t) + d(t) + k\dot{e}(t) \\ &= (k-a)\dot{e}(t) + d(t) - (k-a)\dot{e}(t) - \hat{\beta}\gamma\,\mathrm{sgn}(S) \\ &= d(t) - \hat{\beta}\gamma\,\mathrm{sgn}(S) \end{aligned} \tag{41}$$

Using equation (41) and considering that γ and $\hat{\beta}$ are bounded it is deduced that $\dot{S}(t)$ is bounded.

The second derivative of $V(t)$ can be obtained from equation (38):

$$\ddot{V}(t) = d\,\dot{S}(t) - \beta\,\gamma\frac{d}{dt}|S(t)| \tag{42}$$

Considering that $\dot{S}(t)$ is bounded then it is deduced that $\ddot{V}(t)$ is bounded and therefore $\dot{V}(t)$ is an uniformly continuous function.

Considering that $V(t)$ is bounded and $\dot{V}(t)$ is an uniformly continuous function then from Barbalat's lemma it can be deduced that $\dot{V} \to 0$ as $t \to \infty$. Finally, from equation (41) it is concluded that $S(t) \to 0$ as $t \to \infty$.

When the system reach the sliding mode, $S(t) = 0$, and then from 34:

$$\dot{S}(t) = 0 \quad \Rightarrow \quad \dot{e}(t) = -k\,e(t) \tag{43}$$

Therefore, the tracking error $e(t)$ converges to zero because k is a positive constant.

Finally, using equations (35) and (32) the current command expressed in the synchronously rotating reference frame is obtained:

$$i_{qs}^{e*}(t) = \frac{1}{b}\left[a\,\dot{\theta}_m^* + \ddot{\theta}_m^* + f(t) - (k-a)\,\dot{e} - \hat{\beta}\gamma\,\mathrm{sgn}(S)\right] \tag{44}$$

The semi-global asymptotic stability of the closed-loop system with the proposed sliding mode observers, is provided by the separation principle, which requires the asymptotic stability of the observer fast enough, such that it brings the state estimate close enough to its real value in a short time and restores the stabilizing powers of the controller as a necessary and sufficient condition [22].

V. Continuous approximation of the switching control law

As it is well known the sliding mode control could present the chattering phenomenon because the control signal given by (35) is discontinuous when the system crosses the sliding surface. This involves high control activity and may also excite high-frequency dynamics so that the chattering is not desirable in real applications. The mechanical system inertia will reduce the chattering in the control signal, but undesirable vibrations could appear for some systems with a low mechanical inertia. For these systems, the chattering can be prevented smoothing out the $\mathrm{sgn}(S)$ function that appear in the control signal. In this sense, the $\mathrm{sgn}(S)$ function is replaced by a saturation function in the control law (35):

$$u(t) = -(k-a)\,\dot{e}(t) - \hat{\beta}\gamma\,\mathrm{sat}\left(\frac{S}{\xi}\right) \tag{45}$$

where $sat(\cdot)$ is the saturation function that is defined below:

$$\mathrm{sat}\left(\frac{S}{\xi}\right) = \begin{cases} \mathrm{sgn}(S) & if \quad |S| > \xi \\ \dfrac{S}{\xi} & if \quad |S| \le \xi \end{cases}$$

where ξ is a positive constant

Furthermore, the parameter drift phenomenon may arise in the adaptation of the switching gain β. To avoid this problem, the following modification is performed in the previous adaptive law (36):

$$\dot{\hat{\beta}} = \gamma\,|S_o| \qquad \hat{\beta}(0) = 0 \tag{46}$$

where S_o is defined by:

$$S_o = S - \xi\,\mathrm{sat}\left(\frac{S}{\xi}\right) = \begin{cases} S - \xi & if\ |S| > \xi \\ 0 & if\ |S| \le \xi \end{cases} \tag{47}$$

The control law (45) with the adaptation law (46) leads the rotor mechanical position $\theta_m(t)$ so that the position tracking error $e(t) = \theta_m(t) - \theta_m^*(t)$ can be made as small as desired by choosing an adequately small boundary layer of thickness ξ and the proof is carried out using the Lyapunov stability theory.

$$V(t) = \frac{1}{2}S_o(t)S_o(t) + \frac{1}{2}\tilde{\beta}(t)\tilde{\beta}(t) \tag{48}$$

whose time derivative is given by:

$$\begin{aligned} \dot{V}(t) &= S_o(t)\dot{S}_o(t) + \tilde{\beta}(t)\dot{\tilde{\beta}}(t) \\ &= S_o \cdot [\ddot{e} + k\,\dot{e}] + \tilde{\beta}\dot{\tilde{\beta}} \\ &= S_o \cdot [(k-a)\,\dot{e} + u + d] + (\hat{\beta} - \beta)\gamma|S_o| \\ &= S_o \cdot \left[(k-a)\,\dot{e} - (k-a)\,\dot{e} - \hat{\beta}\gamma\,\mathrm{sat}(S/\xi) + d\right] \\ &\quad +(\hat{\beta} - \beta)\gamma|S_o| \\ &= d\,S_o - \hat{\beta}\gamma|S_o| + \hat{\beta}\gamma|S_o| - \beta\gamma|S_o| \qquad (49) \\ &\le |d||S_o| - (d_{max} + \eta)\gamma|S_o| \\ &\le -\eta\,\gamma|S_o| \le 0 \qquad (50) \end{aligned}$$

The torque current command, $i_{sq}^*(t)$, can be obtained substituting (45) in (32):

$$i_{qs}^{e*}(t) = \frac{1}{b}\left[a\,\dot{\theta}_m^* + \ddot{\theta}_m^* + f(t) - (k-a)\,\dot{e} - \hat{\beta}\gamma\,\mathrm{sat}\left(\frac{S}{\xi}\right)\right] \tag{51}$$

VI. Simulation and Experimental Results

In this section the SMC position regulation performance is analyzed by means of different simulation examples and real test using a commercial induction motor. The block diagram of the proposed control scheme is presented in Figure 1. In this figure, the block 'VSC Controller' represents the proposed adaptive SMC. The block 'limiter' limits the current applied to

This article has been accepted for publication in a future issue of this journal, but has not been fully edited. Content may change prior to final publication. Citation information: DOI 10.1109/TIE.2014.2316239, IEEE Transactions on Industrial Electronics

the motor windings so that it remains within a secure value. The block '$dq^e \rightarrow abc$' makes the conversion between the synchronously rotating and stationary reference frames (Park's Transformation). The block 'Current Controller' consists of a SVPWM current control. The block 'SVPWM Inverter' is a six IGBT-diode bridge inverter with 540 V DC voltage source. The block PI provides the current reference i_{ds}^{e*} from the rotor flux error. The block 'Flux Estimator' represents the proposed sliding mode flux estimator. The block '$\hat{\theta}_e$ Calculation' provides the angular position of the rotor flux vector. Finally, the block 'IM' represents the induction motor.

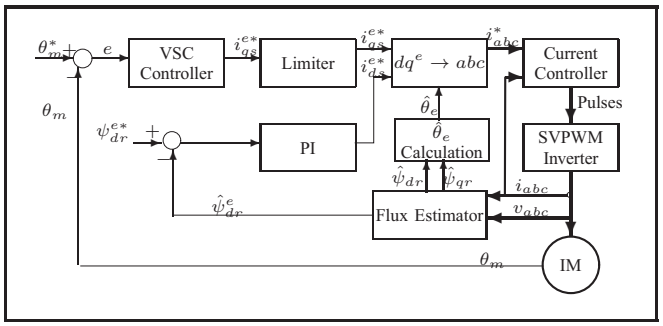

Fig. 1. Block diagram of the proposed sliding-mode field oriented control

In order to carry out the real experimental validation of the proposed control scheme the control platform shown in figure 2 has been designed and constructed.

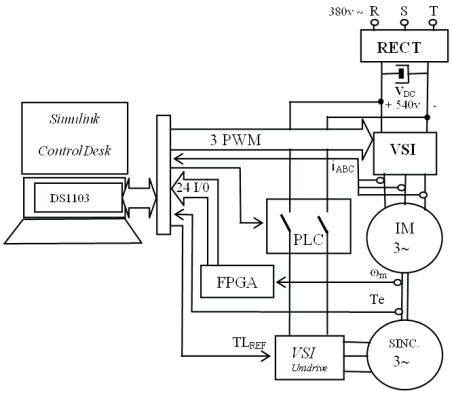

Fig. 2. Block diagram of the induction motor experimental platform

This control platform has been designed in order to test the controller performance in real time using a commercial induction motor. The main elements of this platform are a PC and the DS1103 Controller Board real time interface of dSpace, the power block and the commercial squirrel-cage induction motor, model M2AA 132M4 of $7.5\,kW$ manufactured by ABB. In the PC is running the Windows XP and the software installed is MatLab7/Simulink R14 and ControlDesk 2.7. The power block is formed for a three-phase rectifier connected to 380 V/50 Hz AC electrical net and the inverter formed by a three-phase IGBT/Diode bridge of 50A. Finally, in order to get a DC bus of $540\,V$ a capacitor bank of 27.200 μF is employed. The parameters of this platform are included below:

- w_N : Nominal Speed, 1440 rpm
- T_N : Nominal Torque, 49.3 Nm
- R_s : Resistance of the Stator, 0.81 Ω
- R_r : Resistance of the Rotor, 0.57 Ω
- L_m : Magnetizing Inductance, 0.118 mH
- L_s : Inductance of the Stator, 0.120 mH
- L_r : Inductance of the Rotor, 0.121 mH
- p : Number of Poles, 4
- J : Moment of Inertia, 0.057 $kg\,m^2$
- B : Coefficient of Viscous Friction , 0.015 $Nm/(rad/s)$

The rotor position of this motor is measured using the G1BWGLDBI LTN incremental rotary encoder of 4096 square impulses per revolution. These pulses are quadruplicated in a decoder, giving a resolution of 16384 ppr which gives an angle resolution of 0.000385 rad (0.022 deg).

The PLC is used to ensure that some maneuvers or basic operations, that should be done in the experimental platform, are realized in a safe way. In this sense, the PLC has been programmed in order to control several maneuvers like: start and charge DC bus, discharge DC bus and stop, connection and control of load torque, alarms, etc. The FPGA is programmed in order to calculate the mechanical position and speed of the induction motor using the pulses received from the incremental encoder. The calculation is realized each $100\,\mu s$ and the position and speed values are provided to the PC through the real time target (dS1103). The platform also includes a 190U2 Unimotor synchronous AC servo motor of 10.6 kW connected to the induction motor to generate the load torque (controlled in torque). This servo motor is controlled by its VSI Unidrive inverter module.

The position control is implemented in the experimental platform using a sample time of $100\mu s$. The controller is executed in the real time controller board DS1103 manufactured by dSpace. This controller board includes the PowerPC floating-point processor running at 1MHz and the TMS320F240 DSP that works as slave in order to generate the SVPWM pulses for the inverter. Finally, the algorithms for the position and currents control, the flux and torque estimators, the θ_e angle calculation, the Park's reference frame transformations, the calculations of SVPWM, have been programmed in C language in a Simulink using a S-Builder module which provides a portable and compact code.

The experimental validation is carried out using an uncertainty in the parameters of the system. In this sense, the mechanical parameters used in the controller design are 50% smaller than the real values. The nominal value of the rotor flux is 1.01 Wb and it is obtained for a flux current command value of $i_{sd}^* = 8.61A$. In order to obtain a closed loop flux stabilization, this current reference value is supervised using a PI controller. The gains values for this PI controller has been tuned, and the following values has been obtained $k_p = 150$ and $k_i = 90$.

On the other hand, the electromagnetic torque current command, i_{sq}^*, has been limited to 30 A, in order to provide a protection against overcurrents in the induction motor's stator fed. Finally, the frequency of commutation of VSI module of the platform is limited to 8 kHz.

This article has been accepted for publication in a future issue of this journal, but has not been fully edited. Content may change prior to final publication. Citation information: DOI 10.1109/TIE.2014.2316239, IEEE Transactions on Industrial Electronics

In the examples the values for the controller parameters are: $k = 56$, $\gamma = 10$ and $\xi = 0.05$. These values are experimentally tuned taking into account the influence of this parameters in the controller performance. In the selection of this control parameters the following rules must be taken into account. An increase in the parameter k gives an increase in the position error convergence when the system reach the sliding surface $S(t) = 0$ but this also increases the initial value of the sliding gain $S(t = 0)$ because $S(0) = \dot{e}(0) + ke(0)$, which is undesirable. An increase in the parameter γ gives a faster adaptation of the switching gain but also can increase the final value of the switching gain, which is not desirable. In the selection of the boundary layer of thickness ξ, it should be noted that the smaller the value of ξ is, the smaller is the error but larger is the chattering.

The values for the flux observer parameters are: $g_{i_d} = -44.5$, $g_{i_q} = -44.5$, $g_{\psi_d} = -50$, $g_{\psi_q} = -50$, $k_1 = 100$ and $k_2 = 100$, and the values for the load torque observer parameters are: $k_{w_1} = 25$, $k_{w_2} = 250$ $h_1 = 100$ and $h_2 = 100$. These values are experimentally tuned taking into account the conditions given in equations (6), (11), (16), (22) and (34). In the selection of the observer gains it should be taken into account that a larger values for the observer switching gains may provoke the chattering phenomenon in the observer which is undesirable.

In the first example the IM follows a position reference from 0 to $2\pi\, rad$, and there are several load torque step changes until $T_L = 60\, N.m$, which is a 20% above the nominal torque value (49 Nm). Figure 3 shows the simulation test and figure 4 shows the real test. The first graph shows the reference and the real rotor position, and the second graph shows the rotor position error. As it can be observed the rotor position tracks the desired position in spite of system uncertainties. A little position error can be observed at time $t = 1s$ and $t = 2s$ because there is a torque increment at this time that increase the system uncertainties, and then the controlled system lost the so called sliding mode because the actual sliding gain is too small for this larger uncertainties. However, after a short time, the rotor position error is eliminated because the sliding gain is adapted so that the new sliding gain value can compensate for the new system uncertainty. The third graph shows the d-component of the rotor flux in the stationary reference frame. In this figure it can be observed that the proposed sliding mode observer provides an accurate and fast rotor flux estimation. The fourth graph shows the motor torque, the load torque and the estimated load torque. As it can be seen in this graph, the load torque observer estimates the load torque value accurately. The fifth graph shows the time evolution of the sliding variable. In this figure it can be seen that the system reaches the sliding condition $(S(t) = 0)$ at time $t = 0.25s$, but then the system lost this condition at time $t = 1s$ and $t = 2s$ due to the load torque increment which produces an increment in the system uncertainties. The sixth graph presents the time evolution of the adaptive sliding gain. The sliding gain starts from zero and then it is increased until its value is high enough to compensate for the existing system uncertainties. Then, after $t = 0.5s$, the sliding gain remains constant because the system uncertainties are remained constant as well. Later at time $t = 1s$ and $t = 2s$ the system uncertainties increases due to the increment in the load torque and therefore the sliding gain should be adapted once again in order to overcome this increment in the system uncertainties.

The seventh and the eighth graphs of figure 3, shows the q-component and the d-component of the stator current in the synchronously rotating reference frame. As it can be observed the electromagnetic torque is proportional to the q-component of the stator current because when the field oriented technique is used the electromagnetic torque is proportional to the q-component of the stator current and the rotor flux is proportional to the d-component of the stator current. Finally, in order to show the advantages of the proposed SMO that incorporates a proportional error term in order to improve the observer performance, the last graph of figure 3 shows the rotor flux observer error obtained using the proposed SMO and the traditional SMO that does not includes a proportional error term. As it can be observed the proposed SMO provides better convergence to the real values of the rotor flux.

In the second example the system performance of the proposed controller, using various position reference changes and load torque variations, is presented.

Figure 5 shows the real experiments carried out using the experimental platform. The first graph shows the reference and the real rotor position, and the second graph shows the rotor position error. As it can be observed, after a transitory time, the rotor position tracks the desired position in spite of system uncertainties and position reference variations. The third graph shows the estimated rotor flux. The fourth graph shows the motor torque, the load torque and the estimated load torque. As it can be seen in this graph the proposed load torque observer provides a good estimation of the load torque value. The fifth graph shows the time evolution of the sliding variable. In this figure it can be seen that the system reaches the sliding condition $(S(t) = 0)$ at time $t = 1.05\, s$. Finally, the seventh graph presents the time evolution of the adaptive sliding gain, that increases (when is necessary) in order to overcome the present system uncertainties.

In the third example the performance of the proposed controller considering variations in the stator and rotor resistances is presented. Figure 6, shows the real test of the proposed position control scheme using the experimental platform. In this experimental validation, a variations of 50% in the stator and rotor resistance values are analyzed in order to show the robustness of the proposed control scheme. The variations in the rotor and stator resistance values are implemented in the controller and in the observer algorithms in order to emulate similar variations in the real values of the IM resistances. Therefore, in this experiment the resistance values used in the observer and in the controller are reduced, which emulates an increment of the resistance values in the real system.

The first graph shows the reference and the real rotor position. As it can be observed, after a transitory time, the rotor position tracks the desired position in spite of system uncertainties and stator and rotor resistance variations. The next graph shows the rotor position error. The third graph

This article has been accepted for publication in a future issue of this journal, but has not been fully edited. Content may change prior to final publication. Citation information: DOI 10.1109/TIE.2014.2316239, IEEE Transactions on Industrial Electronics

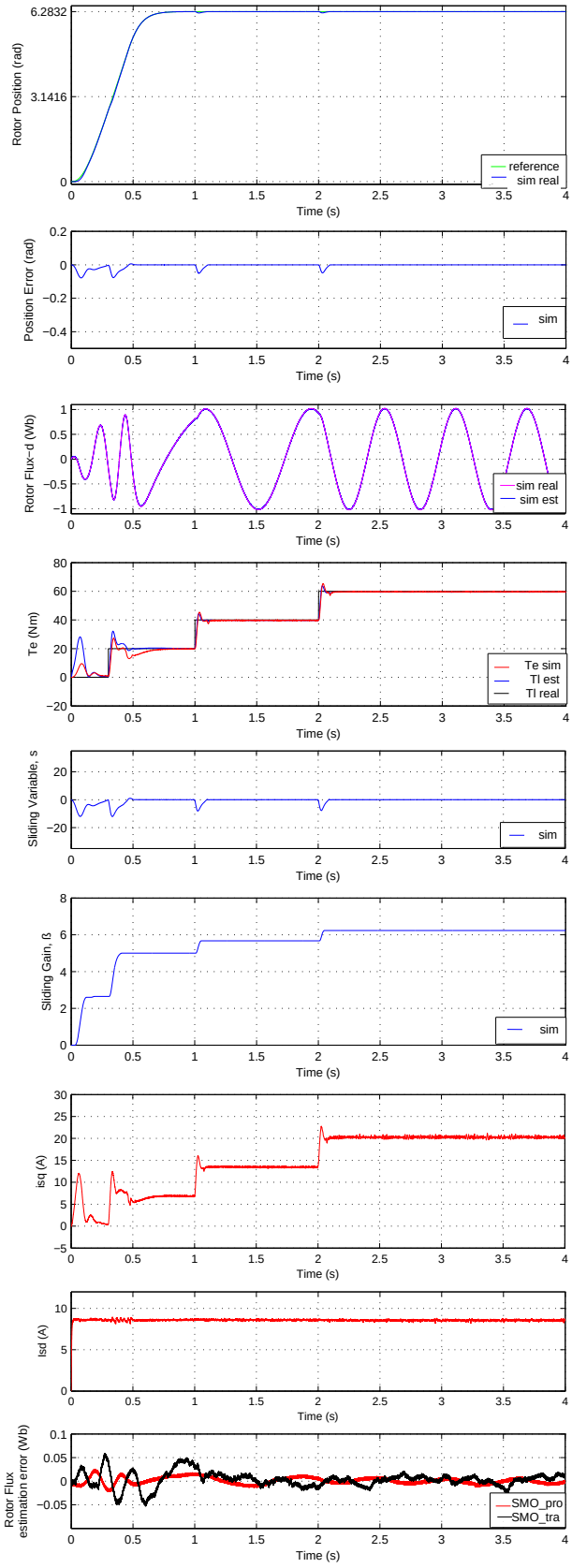

Fig. 3. Position tracking simulation results using a position reference from 0 to 2π and several load torque step changes

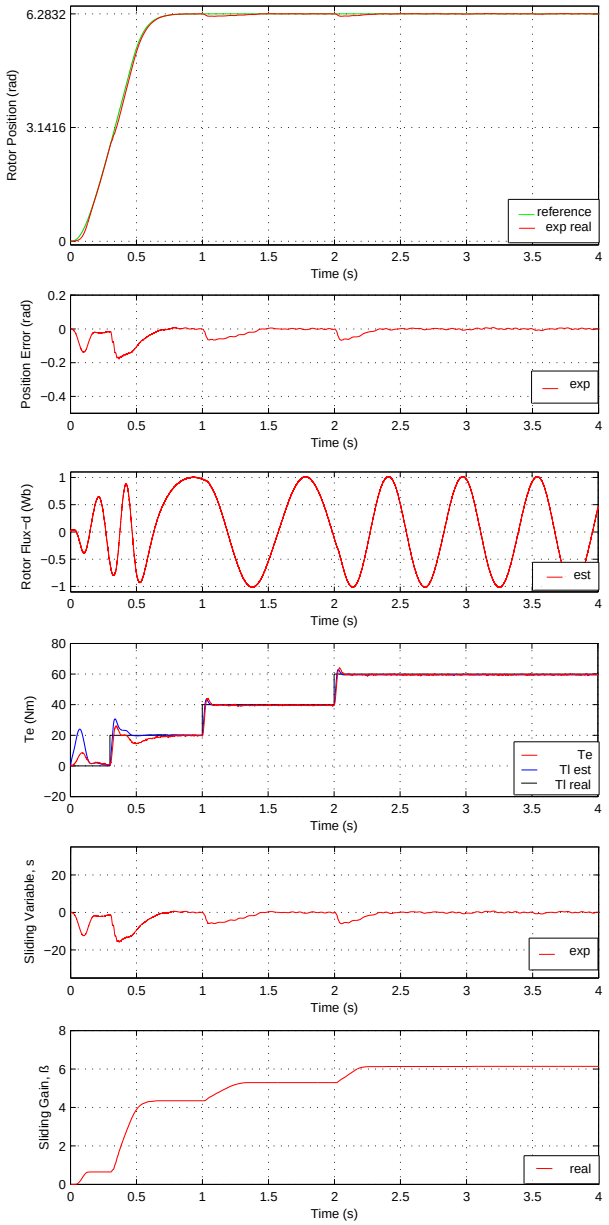

Fig. 4. Position tracking experimental results using a position reference from 0 to 2π and several load torque step changes

shows the rotor speed. As it can be observed the rotor accelerates in order to reach the desired position and then decelerates in order to stop at the desired position. The fourth graph shows the variation of 50% in the value of the stator and rotor resistances that are introduced in the observer and in the controller at time $t = 2\,s$. The fifth graph shows the d-component, the q-component and the module of the estimated rotor flux. As it can be observed the proposed rotor flux estimator presents a good performance under the change of 50% in the stator and rotor resistance value that appears at time $2\,s$. The sixth and the seventh graphs show the d-component and the q-component of the stator current respectively. As it can be observed the stator currents i_{sd} and i_{sq} shows a small changes from time $t = 2\,s$ due to the changes in the rotor and stator resistances. This current variation is greater from

This article has been accepted for publication in a future issue of this journal, but has not been fully edited. Content may change prior to final publication. Citation information: DOI 10.1109/TIE.2014.2316239, IEEE Transactions on Industrial Electronics

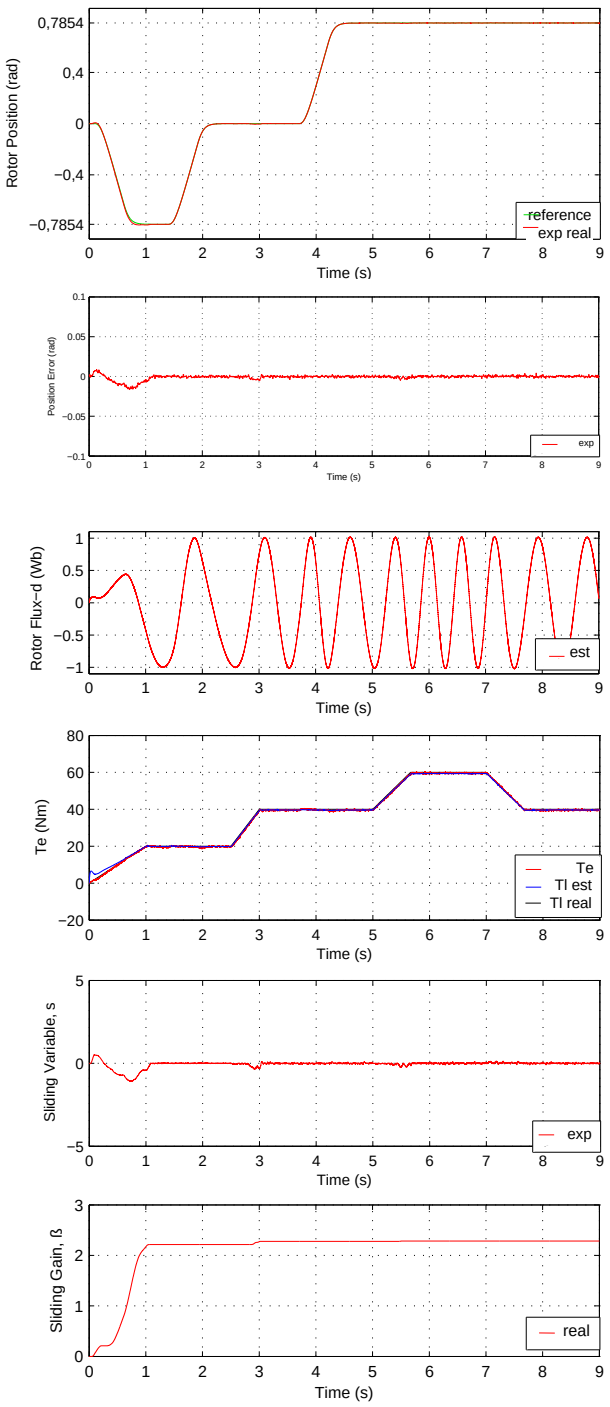

Fig. 5. Position tracking experimental results using several changes in the position reference and several load torque ramp changes

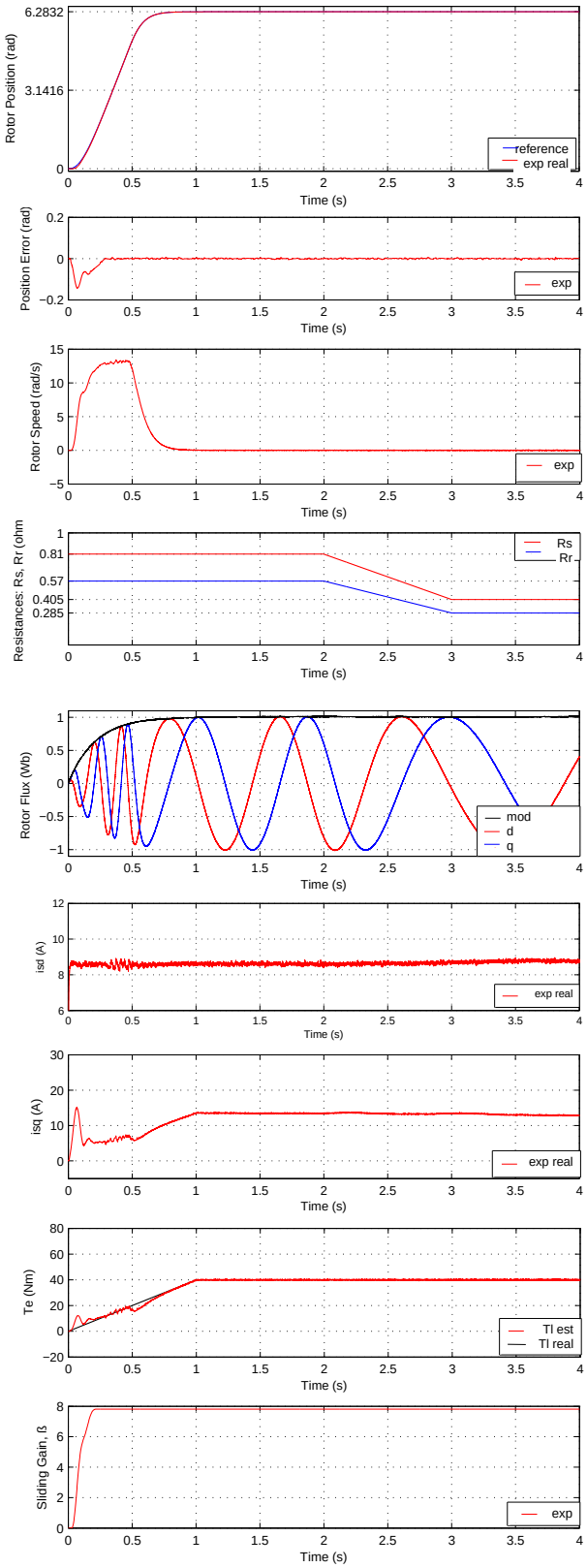

Fig. 6. Position tracking experimental results using a position reference from 0 to 2π, load torque ramp changes and stator and rotor resistance variations

$t = 3\,s$ because the difference between the real resistance values and the resistance values used in the observer and in the controller is also greater. However, as it can be observed in the first graphs the proposed control scheme is robust under these resistance variations and the position tracking is not affected.

The eighth graph shows the real load torque and the estimated load torque. In this graph a change in the estimated load torque can be observed at time $t = 0.47$. This change appears because at this time the motor torque (and also the torque current i_{sq}) decreases in order to reduce the rotor speed value to zero (decelerate). Due to the uncertainties in

the system mechanical inertia, initially, this deceleration is considered by the observer as a load torque variation and then it introduces an error in the value given by the load torque observer. Nevertheless, the proposed control scheme is robust under this observer error and therefore the position tracking performance is not affected. Finally, the ninth graph presents the time evolution of the adaptive sliding gain, that is increased (if is necessary) in order to overcome the system uncertainties.

VII. Conclusion

In this paper an induction motor position regulation using an adaptive SMC for a real-time applications has been presented. The proposed design incorporates an adaptation law for the sliding gain, in order to calculate the appropriate sliding gain value to overcome the system uncertainties. The control signal of this adaptive SMC will be smaller than the control signals of the traditional SMC, because in the last one the sliding gain value should be chosen high enough to overcome all the possible uncertainties that could appear in the system over time. Additionally, in order to avoid the flux sensors a SM rotor flux estimator and load torque observer are proposed to improve the controller performance. Moreover, the proposed observers and the proposed controller do not involve a high computational cost and therefore can be easily implemented in a low cost DSP-processor. Finally, the simulation and real test over a commercial IM, have confirmed that this position control scheme presents a good performance in practice, and that the position tracking objective is achieved under system uncertainties, and also under load torque and resistance variations.

References

[1] D. G. Holmes, B. P. McGrath, and S. G. Parker, "Current Regulation Strategies for Vector-Controlled Induction Motor Drives", *IEEE Trans. Ind. Electron.*, vol. 59, no. 10, pp. 3680-3689, Oct. 2012.

[2] J. Guzinski and H. Abu-Rub, "Speed Sensorless Induction Motor Drive With Predictive Current Controller", *IEEE Trans. Ind. Electron.*, vol. 60, no. 2, pp. 669-709, Feb. 2013.

[3] P. Alkorta, O. Barambones, J.A. Cortajarena, and A. Zubizarrreta, "Efficient Multivariable Generalized Predictive Control for Sensorless Induction Motor Drives", *IEEE Trans. Ind. Electron.*, vol. 61, no. 9, pp. 5126-5134, Sep. 2014.

[4] T. Orłowska-Kowalska, M. Dybkowski and K. Szabat, "Adaptive Sliding-Mode Neuro-Fuzzy Control of the Two-Mass Induction Motor Drive Without Mechanical Sensors", *IEEE Trans. Ind. Electron.*, vol. 57, no. 2, pp. 553-564, Feb. 2010.

[5] H. Sira-Ramrez, F. Gonzlez-Montaez,J.A. Corts-Romero, and A. Luviano-Jurez, "A Robust Linear Field-Oriented Voltage Control for the Induction Motor: Experimental Results", *IEEE Trans. Ind. Electron.*, vol. 60, no. 8, pp. 3025-3033, August. 2012.

[6] M. Suetake, I. N. da Silva, and A. Goedtel, "Embedded DSP-Based Compact Fuzzy System and Its Application for Induction-Motor V/f Speed Control", *IEEE Trans. Ind. Electron.*, vol. 58, no. 3, pp. 750-760, Mar. 2011.

[7] L. Zheng, J. E. Fletcher, B. W. Williams, and X. He, "A Novel Direct Torque Control Scheme for a Sensorless Five-Phase Induction Motor Drive", *IEEE Trans. Ind. Electron.*, vol. 58, no. 2, pp. 503-513, Feb. 2011.

[8] M. Comanescu, "An Induction-Motor Speed Estimator Based on Integral Sliding-Mode Current Control", *IEEE Trans. Ind. Electron.*, vol. 56, no. 9, pp. 3414-3423, Sep. 2009.

[9] A. Sabanovic "Variable Structure Systems With Sliding Modes in Motion Control", *IEEE Trans. Indus. Informatics*, vol. 7, pp.212-223. May. 2011.

[10] LX Zhang, "Sensorless Induction Motor Drive Using Indirect Vector Controller and Sliding-Mode Observer for Electric Vehicles", *IEEE Trans. Ind. Electron.*, vol. 62, no. 7, pp. 3010-3018, Sep. 2013.

[11] C. Cecati, "Position Control of the Induction Motor Using a Passivity-Based Controller", *IEEE Trans. Ind. Applications.*, vol. 60, no. 2, pp. 1277-1284, Sep./Oct. 2000.

[12] B. Veselić, B. Peruničić-Draženović, and Č. Milosavljević, "High-Performance Position Control of Induction Motor Using Discrete-Time Sliding-Mode Control", *IEEE Trans. Ind. Electron.*, vol. 55, no. 11, pp. 3809-3817, Nov. 2008.

[13] F. Betin and G.-A. Capolino, "Shaft Positioning for Six-Phase Induction Machines With Open Phases Using Variable Structure Control", *IEEE Trans. Ind. Electron.*, vol. 59, no. 6, pp. 2612-2620, Jun. 2012.

[14] O. Barambones, P. Alkorta, J. M. Gonzalez de Durana and E. Kremers, "A Robust Position Control for Induction Motors using a Load Torque Observer", *20th Mediterranean Conference on Control & Automation (MED)*, Barcelona, Spain, Jul. 3-6, 2012.

[15] D. Chatterjee, "A Simple Leakage Inductance Identification Technique for Three-Phase Induction Machines Under Variable Flux Condition", *IEEE Trans. Ind. Electron.*, vol. 59, no. 11, pp. 4041-4048, Nov. 2012.

[16] M. Barut, Member, R. Demir, . Zerdali, and R. Inan, "Real-Time Implementation of Bi Input-Extended Kalman Filter-Based Estimator for Speed-Sensorless Control of Induction Motors", *IEEE Trans. Ind. Electron.*, vol. 59, no. 11, pp. 4197-4206, Nov. 2012.

[17] T. Orłowska-Kowalska and M. Dybkowski, "Stator-Current-Based MRAS Estimator for a Wide Range Speed-Sensorless Induction-Motor Drive", *IEEE Trans. Ind. Electron.*, vol. 57, no. 4, pp. 1296-1308, Apr. 2010.

[18] S. Jafarzadeh, C. Lascu, and M.S. Fadali, "State Estimation of Induction Motor Drives Using the Unscented Kalman Filter", *IEEE Trans. Ind. Electron.*, vol. 59, no. 11, pp. 4207-4216, Nov. 2012.

[19] Z. Xu, M.F. Rahman, "Comparison of a Sliding Observer and a Kalman Filter for Direct-Torque-Controlled IPM Synchronous Motor Drives", *IEEE Trans. Ind. Electron.*, vol. 59, no. 11, pp. 4179-4188, Nov. 2012.

[20] Z. Qiao, T. Shi, Y. Wang, Y. Yan, C. Xia, X. He, "New Sliding-Mode Observer for Position Sensorless Control of Permanent-Magnet Synchronous Motor", *IEEE Trans. Ind. Electron.*, vol. 60, no. 2, pp. 710-719, Feb. 2013.

[21] P.V. Kokotovic, H. Khalil, J. OReilly. (1996) Singular Perturbation Methods in Control: Analysis and Design *Academic Press*, New York.

[22] A. N. Atassi, H. K. Khalil. (2000) Separation results for the stabilization of nonlinear systems using different high-gain observer designs, *Systems & Control Letters*, Vol. 39, pp.183-191.

Oscar Barambones (M'07-SM'13) received the M.Sc. degree in applied physics (specialty in electronics and automatic control) and the Ph.D. degree from the Faculty of Science and Technology of Leioa, University of the Basque Country (UPV/EHU), Leioa, Spain, in 1996 and 2000, respectively. He currently teaches in the Department of Systems Engineering and Automatics, School of Engineering of Vitoria, UPV/EHU, Vitoria-Gasteiz. His main research interests are induction machine drives, speed control, position control, variable structure control, and predictive control.

Patxi Alkorta (M'12) received the B.S. degree in electronics engineering (specialty in automatic control) from the Faculty of Science and Technology of Leioa, University of the Basque Country (UPV/EHU), Leioa, Spain, in 2004 and the Ph.D. degree in robotics and automatic control systems from UPV/EHU, Faculty of Engineering of Bilbao, in 2011. He currently teaches in the Department of Systems Engineering and Automatics, School of Engineering of Eibar, UPV/EHU, Eibar. His main research interests are induction motor drives, speed and position control, variable structure control, and predictive control.